EXAMINATION OF EFFECTIVE LENGTH FACTOR FOR RC COLUMNS IN NON-SWAY FRAMES

S. Ali Mirza
Lakehead University, Canada

Timo K. Tikka
Stantec Consulting, Canada

ABSTRACT

The Canadian Standards Association (CSA) Standard for Design of Concrete Structures (A23.3-04) permits the use of moment magnifier method for computing the design ultimate strength of slender reinforced concrete (RC) columns that are part of non-sway frames. This computed strength is influenced by the column effective length factor K, effective flexural stiffness EI, and equivalent uniform bending moment diagram factor C_m among others. Previous investigations by the authors examined the equations available in literature for computing EI and C_m factor. For this study, nearly 3000 simple non-sway reinforced concrete frames subjected to short-term loads were simulated and used to investigate the effect of using different equations for the effective length factor K when computing the strength of columns in these frames by the moment magnifier approach. An elaborate theoretical model was developed and used for computing the ultimate strength of columns in simulated frames. The theoretically computed column ultimate strengths were compared to the ultimate strengths of the same columns computed from the CSA moment magnifier method using selected equations for K available in literature. For the purpose of analysis, the theoretically computed strengths were divided by the CSA strengths to obtain the so-called strength ratios. The statistical analyses of strength ratios presented in this paper show that, for computing the CSA ultimate strength of columns in non-sway frames, the current practice of using Jackson-Moreland Alignment Chart is the most accurate method for determining the effective length factor.

Keywords: Building codes; concrete structures; effective length; non-sway frames; slender columns.

1. INTRODUCTION

In non-sway frames, structural members framing into the ends of a column influence its strength. Such a column is subjected to axial load and equal or unequal end moments, which are caused by unbalanced beam loads, and deflects laterally between the column ends due to the presence of end moments. The axial load acting through this lateral deflection causes additional (second-order) bending moments along the column height. The second-order bending moments cause additional rotation of the column ends as well as the additional rotation of the members framing into the column. This, in turn, results in changes to the initial bending moments at the ends of the column and to the beam bending moments computed from a conventional elastic frame analysis.

CSA A23.3-04 (2004) permits the use of a moment magnifier approach to approximate the second-order moments due to the axial load acting through the lateral deflection caused by the end moments acting on a column. For this method, the larger of the column end moments (M_2), computed from a conventional elastic frame analysis, is magnified to include the second-order effects. The second-order effects on columns in non-sway frames are functions of the larger end moment (M_2) in addition to the column effective length factor (K), effective flexural stiffness (EI), equivalent uniform bending moment diagram factor (C_m), applied axial load (P_u), and sustained load factor (β_d), which is neglected for short-term loads. Earlier studies by the authors examined the C_m and EI equations available in the literature. The research reported here conducts a similar examination of the available K equations.

Almost 3000 simple reinforced concrete (RC) frames in the shape of an inverted T, shown in Figure 1, were simulated to evaluate the influence of the effective length factor K used in the moment magnifier method for determining the ultimate strength of columns that were part of non-sway frames subjected to short-term loads. The theoretically computed column ultimate strengths were compared to the ultimate strengths computed from the moment magnifier method using different equations for K. The beams framing into the columns were subjected to pattern loads causing varying beam bending moments and column end moments. For two load cases, Load Cases 5 and 6 shown in Figure 1, the top end of the column was also subjected to an applied bending moment. The study concentrates on the examination of equations for the column effective length factor K specified in the Explanatory Notes on CSA A23.3-04 (Jackson-Moreland Alignment Chart) (CAC 2006) and K proposed by Duan et al. (1993). These equations for K are used for computing the column slenderness effect from the CSA moment magnifier approach. A more detailed examination by the authors of the CSA moment magnifier is currently under study.
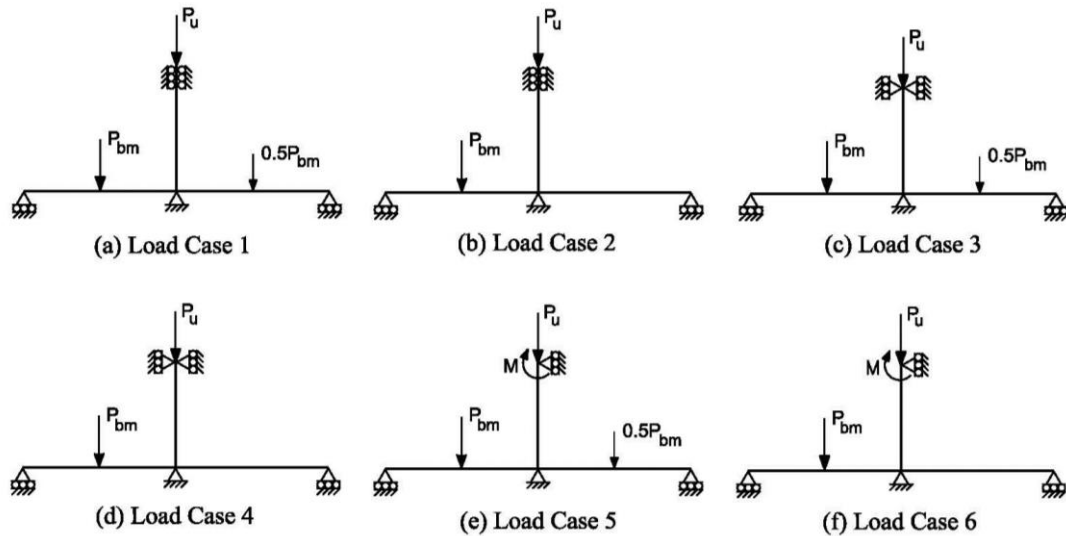

Figure 1: Frame configurations and load cases used for this study

2. THEORETICAL STRENGTH MODEL

A non-linear second-order frame analysis procedure was developed to analyze reinforced concrete columns that are part of frames. In order to account for second-order effects due to geometric and material nonlinearities, the theoretical model (computer software) uses: (a) classical stiffness analysis of linear elastic two-dimensional structural frames; (b) iterative technique combined with an incremental method for computing load-deflection behavior and failure load of the frame; (c) frame discretization to account for column chord (P-Δ) effects; and (d) axial load-bending moment-curvature (P-M-ϕ) relationships to account for effects of non-linear material behaviour.

A theoretical cross section strength subroutine was used to compute the P-M-ϕ relationships for a given cross section using force equilibrium and strain compatibility solution. The major assumptions used in determining the P-M-ϕ relationships were: (a) strains between concrete and reinforcing steel were compatible and no slip occurred; (b) the strain was linearly proportional to the distance from the neutral axis; (c) concrete and steel stresses were functions of strains; (d) deflections were small, such that curvatures could be calculated as the second derivative of the deflection; (e) shear stresses were small and their effect on the strength could be neglected; and (f) the confinement of concrete provided by lateral ties was considered. A reinforced concrete column cross section was assumed to consist of two materials, concrete and longitudinal reinforcing steel. The concrete was divided into three types, unconfined and partially confined concretes outside and inside the lateral ties, respectively, and highly confined concrete inside the beam-to-column joints. A modified Kent-and-Park (Park et al. 1982) stress-strain relationship was used for concrete in compression. A second-order parabola described the ascending portion of the curve up to the maximum stress and a straight line defined the descending branch of the curve beyond the maximum stress. The slope of the descending branch for the unconfined concrete depended on the concrete strength. For the partially confined concrete, the slope of the descending branch was affected by the concrete strength as well as the

level of confinement provided by lateral ties. The stress-strain relationship for the highly-confined concrete was described by an ascending second-order parabola to the peak stress and then maintained as a constant at all strains beyond the one corresponding to the peak stress. The tension stiffening of concrete was represented by an ascending linear, stress-strain relationship with maximum tensile stress represented by the modulus of rupture fr, as suggested by Mirza and MacGregor (1989), and beyond maximum tensile stress by a linear descending branch as suggested by Bazant and Oh (1984). An elastic-plastic-strain hardening stress-strain relationship was used for the reinforcing steel in tension and compression. In addition, strength reduction due to the buckling of longitudinal reinforcing steel in compression was considered in the theoretical procedure, as suggested by Yalcin and Saatcioglu (2000).

The frame was discretized into a specified number of elements between nodes (member ends) to permit the frame analysis procedure to account for the second-order member or chord effects (P-Δ) due to axial loads acting through the deformed column(s). The lengths of these elements were equal to the depths of beam and column cross sections. The theoretical model permitted the selected nodal or joint loads to be incremented while other loads were maintained at a constant level. For each increment of loads used for the prescribed loading configuration, the second-order displacements were evaluated using the flexural stiffness of each element and a two-dimensional frame analysis procedure. The element flexural stiffness for each load increment and displacement iteration was computed as $EI = M/\phi$ using the basic strength of material concepts applied to members subjected to small deflections. For a given axial load the M-ϕ relationship was known. The loads in the prescribed configuration were incremented until the theoretical failure load was reached. The theoretical failure load was defined as a set of maximum stable forces applied externally to the frame that were in equilibrium with the internal forces within the frame. Note that special modelling techniques were used for the frames at beam-to-column joints to account for the additional strength resulting from the concrete confinement at and near the joints. Further details of the theoretical strength model are documented elsewhere (Tikka and Mirza 2014).

The strengths and load-deflection behaviours of 13 non-sway reinforced concrete test frames subjected to short-term loads were taken from the published literature (Breen and Ferguson 1964; Furlong and Ferguson 1966; and Blomeier and Breen 1975) and used to check the accuracy of the theoretical model. The strength comparisons represented the ultimate tested-to-computed strengths (strength ratios) with no resistance factors applied to the computed strengths or computed load-deflection curves. The average value, coefficient of variation, minimum value, and maximum value of the strength ratios were calculated as 1.02, 0.11, 0.81, and 1.19, respectively, for these frames. The plotted load-deflection curves (not shown here) compared the measured lateral deflections at the mid-height of the column with the theoretically computed lateral deflections for all frame tests examined. It was found that the shape of the theoretically computed load-deflection curves followed or ran closely parallel to the shape of the measured load-deflection curves. From the strength comparisons, strength ratio statistics and load-deflection curves, it was evident that the theoretical model developed here computed the strength of reinforced concrete columns in non-sway frames with reasonable accuracy.

3. DESCRIPTION OF SIMULATED REINFORCED CONCRETE NON-SWAY FRAMES

For the analysis of simulated reinforced concrete non-sway frames used in this study, the cross section properties of the columns and beams were kept constant. The lower end of a column having a gross cross section of 305 mm × 305 mm (Figure 2(a)) was framed rigidly into two beams of equal spans having a cross section of 305 mm wide by 610 mm deep (Figure 2(b)). Note that a previous study showed that a smaller cross section size was more critical for investigating the strength of slender reinforced concrete columns (Mirza and McGregor 1989). Hence, the overall dimensions of 305 mm × 305 mm were chosen for the column cross section. Similarly, the column longitudinal reinforcing steel ratio (ρ_{col}) in simulated frames was kept at about 2%, which is within the lower one-third of the usual range of 1 to 4% used for ρ_{col}. Note that concrete columns with light longitudinal reinforcing are more critical for investigating the strength (Mirza and MacGregor 1989). The nominal compressive strength of concrete (f'_c) and yield strength of reinforcing steel (f_y) were taken as 34.5 MPa and 414 MPa, respectively. These values of f'_c and f_y were selected because they are most commonly used in low-rise buildings.

The variables studied to examine the effective length factor used in the CSA A23.3-04 moment magnifier approach for columns in reinforced concrete non-sway frames are as follows: (a) The load patterns, the end conditions at the top of the column, and the end moment applied to the upper end of the column producing 6 different load cases (Figure 1); (b) the slenderness ratio of the column (ℓ_{col}/h_{col}), where ℓ_{col} = unsupported height of the column,

h_{col} = overall thickness of the column cross section; (c) the slenderness ratio of the beams (ℓ_{bm}/h_{bm}), where ℓ_{bm} = unsupported length of the beam, h_{bm} = overall thickness of the beam cross section; and (d) the magnitude of the beam loading controlled by the ratio of the beam applied bending moment to the yield bending moment ($M_{bm}/M_{y(bm)}$), where the yield bending moment is defined as the bending moment acting on the beam cross section at the onset of initial yielding of the beam flexural tension steel and computed from CSA A23.3-04 without using the resistance factors. Specified values of variables used for this study are given in Table 1. Note that variations in column and beam slenderness ratios and column upper end conditions (pin-ended or fix-ended) produced a range of effective lengths that permitted the evaluation of the effective length factor (K). Some combinations of the column and beam slenderness ratios listed in Table 1 produced impractical frames. However, all simulated columns for which theoretically computed δns values were greater than 1.0 were included in the analysis. This permitted the examination of higher ranges of relative column stiffnesses and the resulting K factors than would have been otherwise possible. Table 1 also indicates that the magnitude of the beam loads shown in Figure 1 was varied to study the effect of yielding of the flexural tension reinforcing steel in the beams. The beam loads were applied so that the maximum computed bending moment in one of the beams was equal to the predefined moment that ranged from $0.84M_{y(bm)}$ to $1.12M_{y(bm)}$ (Table 1), representing conditions at or near ultimate loads. Note that the ratio of the ultimate bending moment resistance to yield bending moment for the beam cross section, shown in Figure 2(b), was computed from CSA A23.3-04 (without the resistance factors) as 1.12. The M_1/M_2 ratio for columns in frames used in this study varied from -0.5 to 1.0.
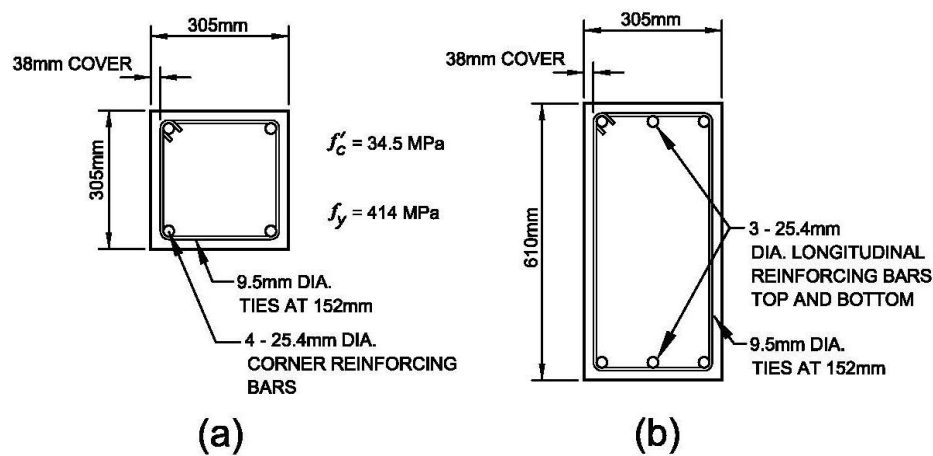

Figure 2: Member properties used for analysis of simulated reinforced concrete frames: (a) column cross section; and (b) beam cross section

4. THEORETICAL ULTIMATE STRENGTH OF COLUMNS IN SIMULATED NON-SWAY FRAMES

To determine the theoretical axial load strength ($P_{u(th)}$) of a column, the axial load was incremented to the failure load starting from an axial load equal to 10 percent of the concentric axial load strength of the column cross section. For each level of axial load under consideration, the maximum bending moment along the column length was computed. The non-linear second-order analysis (theoretical strength model described in an earlier section) was used for this purpose. The bending moments along the length of the beams were checked to ensure that the beam bending moment ratio ($M_{bm}/M_{y(bm)}$) was at the predefined level (Table 1). If the beam bending moments did not correspond to the desired beam bending moment ratio, the beam loads were adjusted to maintain the desired level of $M_{bm}/M_{y(bm)}$ ratio. The bending moments in the beams were monitored to ensure also that the failure of the column took place prior to the failure of a beam. If the failure of one of the beams occurred before the column failure, the beam loads were adjusted and the entire process was repeated. For load cases 5 and 6 (Figure 1), the moment at the top end of the column was applied proportionally to the axial load to maintain the predefined end eccentricity that corresponded to one of the $M/P_u h$ values given in Table 1. Therefore, the applied bending moment at the top end of the column increased at the same rate as the axial load. The first-order end moment ratio (M_1/M_2) and end eccentricity ratio ($e/h = M_2/P_{u(th)}h$) were computed along with $P_{u(th)}$ for the column in the frame under consideration and were used in analyses presented in the later part of this paper.

Table 1: Specified Properties of Simulated Reinforced Concrete Frames

Load Cases	Properties	Specified Values	Number of Specified Values
1 and 2[a] Upper end of column fixed against rotation, as shown in Fig. 1(a) and 1(b)	ℓ_{col}/h_{col}	15; 17.5; 20; 22.5; 25; 27.5; 30; 32.5; 35; 37.5; 40; 42.5; 45; 47.5; 50; 52.5; 55	17
	ℓ_{bm}/h_{bm}	10; 15; 20; 30; 40	5
	$M_{bm}/M_{y(bm)}$	0.84; 1.00; 1.06; 1.12	4
3 and 4[b] Upper end of column pin-ended, as shown in Fig. 1(c) and 1(d)	ℓ_{col}/h_{col}	10; 12.5; 15; 17.5; 20; 22.5; 25; 27.5; 30; 32.5; 35; 37.5; 40; 42.5; 45	15
	ℓ_{bm}/h_{bm}	10; 15; 20; 30; 40	5
	$M_{bm}/M_{y(bm)}$	0.84; 1.00; 1.06; 1.12	4
5 and 6[c] Bending moment applied to upper end of column that is pin-ended, as shown in Fig. 1(e) and 1(f)	ℓ_{col}/h_{col}	15; 20; 25; 30; 35; 40	6
	ℓ_{bm}/h_{bm}	10; 15; 20; 30; 40	5
	$M_{bm}/M_{y(bm)}$	0.84; 1.00; 1.06; 1.12	4
	$M/(P_u h)$	0.1; 0.2; 0.3; 0.4; 0.6; 0.8; 1.0	7

[a]Total number of simulated frames equals ($17\times5\times4=$) 340 for each of Load Cases 1 and 2.
[b]Total number of simulated frames equals ($15\times5\times4=$) 300 for each of Load Cases 3 and 4.
[c]Total number of simulated frames equals ($6\times5\times4\times7=$) 840 for each of Load Cases 5 and 6.
Note: Each simulated frame had a different combination of specified properties shown above with $f'_c = 34.5$ MPa and $f_y = 414$ MPa.

5. DESIGN ULTIMATE STRENGTH OF COLUMNS IN SIMULATED NON-SWAY FRAMES

5.1 CSA A23.3-04 Moment Magnifier Method

The first step for computing the CSA ultimate strength of a slender column in a non-sway frame is to determine the cross section strength, which is represented by an axial load-bending moment (P-M) strength interaction diagram. The cross section strength interaction diagram was defined by 102 points, which were computed using the compatibility of strains and the equilibrium of forces acting on the cross section. For computing the CSA cross section strength, it was assumed that (a) the strains were linearly proportional to the distances from the neutral axis; (b) the maximum concrete strain $\varepsilon_{cu} = 0.0035$ existed at the extreme compression fiber; (c) the compressive stress in concrete was represented by a rectangular stress block as defined by CSA A23.3-04; (d) the specified concrete strength was used for computing the maximum concrete stress in the stress block; and (e) the concrete was assumed to have no strength in tension. The material and member resistance factors (ϕ_c, ϕ_s, ϕ_m) were taken equal to 1.0.

The CSA moment magnifier procedure for slender columns uses the moment magnifier δ_{ns} and the larger of the two column end moments M_2 obtained from a conventional elastic frame analysis to compute the magnified moment M_c (M_{max}), which includes second-order effects occurring along the height of the column:

[1] $M_{max} = M_c = \delta_{ns}M_2 = C_m\delta_1M_2 \geq M_2$

In Eq. 1, δ_{ns} is the moment magnifier for a column in a non-sway frame; M_2 is the larger of the two factored end moments (M_1 and M_2) computed from a conventional elastic frame analysis and is always taken as positive; C_m is the equivalent uniform bending moment diagram factor; δ_1 is the moment magnifier for the same column when subjected to axial load and equal and opposite (equivalent) end moments causing symmetrical single curvature bending and is calculated from $1/(1-(P_f/\phi_mP_c))$; P_f is the applied factored axial load (ultimate axial load resistance P_u) under consideration; ϕ_m is the member resistance factor taken as 1.0; P_c is the critical buckling load computed from $\pi^2EI/(K\ell)^2$; EI is the effective flexural stiffness; K is the effective length factor; and ℓ is the length of the

column. The Explanatory Notes on CSA A23.3-04 (CAC 2006) permit the use of the Jackson-Moreland Alignment Chart, which is based on Eq. 2, for determining the effective length factor K for columns in non-sway frames:

[2] $$\frac{G_A G_B}{4}\left(\frac{\pi}{K}\right)^2 + \left(\frac{G_A + G_B}{2}\right)\left(1 - \frac{\pi/K}{\tan(\pi/K)}\right) + \frac{2\tan(\pi/2K)}{(\pi/K)} - 1 = 0$$

In Eq. 2, G_A and G_B are the relative stiffnesses of the column at upper and lower joints, respectively, and were computed as the ratios of the sum of stiffnesses of columns ($\sum(EI/\ell)_{col}$) meeting at joint A or B to the sum of stiffnesses of beams ($\sum(EI/\ell)_{bm}$) meeting at the same joint. For G_A and G_B, EI values were taken as $0.7E_cI_{g(col)}$ and $0.35E_cI_{g(bm)}$ for columns and beams, respectively, as permitted by CSA A23.3-04, where E_c = modulus of elasticity of concrete, and $I_{g(col)}$, $I_{g(bm)}$ = moments of inertia of the column and beam gross cross sections, respectively. For frames used in this study (Figure 1), the upper end of the column (Joint A) has no beams framing into it. The upper end of the column is either pin-ended or fix-ended and, therefore, G_A is theoretically infinity or zero, respectively. To avoid numerical problems in solving Eq. 2, G_A was set equal to 1000 when the upper end of the column was pin-ended and taken as 0.001 when the upper end of the column was fix-ended.

Equation 1 was used to obtain the bending moment resistance of a column in a frame for a given level of axial load (P_u) directly from the cross section strength interaction diagram. To do this, the cross section bending moment resistance (M_{cs}) was substituted for the magnified column moment (M_c) in Eq. 1. Then, the larger of the two end moments (M_2), which can be applied to the column at the given axial load P_u, was computed by solving Eq. 1 for M_2 = M_c/δ_{ns} = M_{cs}/δ_{ns}. Note that the maximum axial load that can be applied to a slender column is less than the pure axial load resistance of the cross section P_o ($P_{r,max}$ permitted by CSA A23.3-04 without ϕ factors) and is also less than the column critical load resistance P_c. Hence, the points on a column strength interaction curve were generated for P_u values that were lower than both P_o and P_c. For a desired M_1/M_2 ratio, M_2 values were computed from the procedure described above for all levels of axial load (P_u) that were lower than or equal to both P_o and P_c. This generated the column axial load-bending moment interaction diagram for the M_1/M_2 ratio under consideration. Repeating the step for all desired M_1/M_2 ratios generated a series of column strength interaction curves. The CSA axial load strength ($P_{u(des)}$) of a column was then computed from linear interpolation of points on these interaction diagrams, using the first order M_1/M_2 and e/h ratios determined earlier for that column from the theoretical procedure described in the preceding section.

5.2 Modified CSA Moment Magnifier Method with Alternative Equation for K Factor

Duan et al. (1993) proposed a simple equation for computing the effective length factor for columns in non-sway frames:

[3] $$K = 1 - \frac{1}{5 + 9G_A} - \frac{1}{5 + 9G_B} - \frac{1}{10 + G_A G_B}$$

In addition, the Commentary to ACI 318-05 (2005) permitted the use of expressions proposed by Cranston (1972), where K was taken as the smaller of the following for columns in non-sway frames:

[4a] $$K = 0.7 + 0.05(G_A + G_B) \leq 1.0$$

[4b] $$K = 0.85 + 0.05G_{min} \leq 1.0$$

In Eq. 4b, G_{min} was the smaller of G_A and G_B. A comparison of K computed from Eq. 2 (Jackson-Moreland Alignment Chart), Eq. 3 (Duan et al. 1993), and Eq. 4 (Cranston 1972) is shown in Figure 3. The following observations are made from Figure 3: (a) Cranston's expressions produce effective length factors that are very conservative compared to the values obtained from the Jackson-Moreland Alignment Chart when the upper joint is fix-ended ($G_A = 0$); (b) Duan's equation produces effective length factors that are almost the same as those obtained from the Jackson-Moreland Alignment Chart when the upper joint is fix-ended ($G_A = 0$); and (c) when the upper joint is pin-ended ($G_A = \infty$), both Duan's and Cranston's equations produce conservative results compared to the effective length factor computed from the Jackson-Moreland Alignment Chart. To investigate the effect of the K

factor computed from Duan et al. (1993) on the strength of slender reinforced concrete columns, Eq. 3 was used in place of Eq. 2 and the rest of the moment magnifier procedure described previously was followed. No further analysis was performed with Cranston's equation (1972), because it produced very conservative values of K for fix-ended columns in Figure 3(a) and similar values of K as those produced by the Duan et al. equation for pin-ended columns in Figure 3(b).
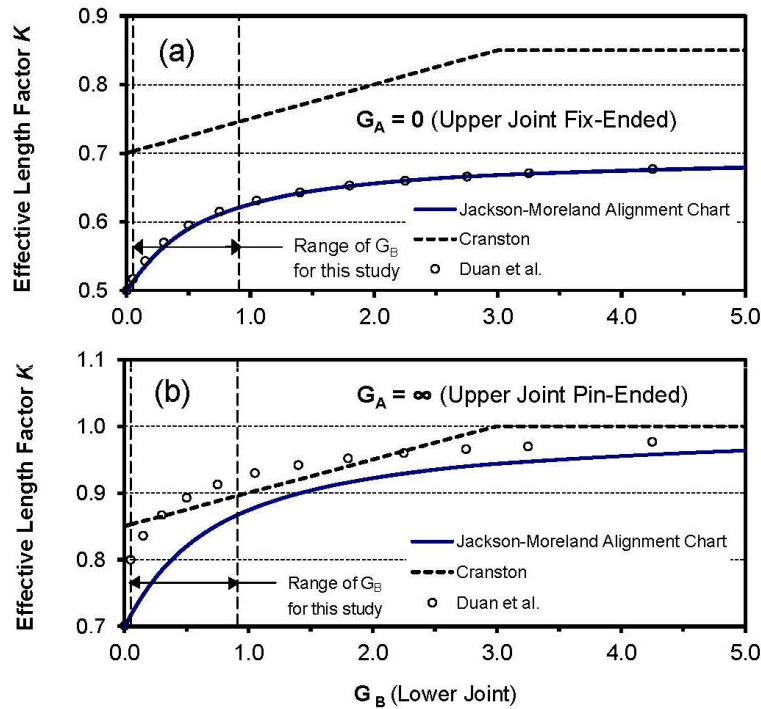

Figure 3: Comparison of effective length factors (K) computed from different design equations when (a) the upper joint of the column is fix-ended; and (b) the upper joint of the column is pin-ended

6. STRENGTH RATIOS FOR COLUMNS IN SIMULATED NON-SWAY FRAMES

To evaluate the effective length factor used in the moment magnifier approach for determining column strength, 2960 simple reinforced concrete frames were simulated. The cross section and material properties of columns and beams used in these frames are shown in Figure 2. The combinations of support conditions and applied loads produced six different load cases (Figure 1). Each frame had a different combination of column slenderness ratio, beam slenderness ratio, support condition, and beam loads (Table 1). The column theoretical ultimate strengths ($P_{u(th)}$) were computed from the procedure outlined in a previous section. The column design ultimate strengths $P_{u(des)}$ were calculated from the design procedures described in the preceding section using Eq. 2 (Jackson-Moreland Alignment Chart) or Eq. 3 (Duan et al. 1993) for the effective length factor K used in the computation of P_c. Note that ϕ_c, ϕ_s, and ϕ_m factors were taken equal to 1.0 for computing $P_{u(des)}$. Finally, the strength ratios were computed by dividing $P_{u(th)}$ by $P_{u(des)}$, and were statistically analyzed to examine and evaluate the equations for effective length factor K. These analyses and evaluations are presented in the sections that follow.

7. EXAMINATION OF STRENGTH RATIOS FOR COLUMNS IN SIMULATED NON-SWAY FRAMES

Only the columns where the theoretically computed maximum magnified bending moment due to second-order effects along the height of the column was greater than the larger first-order end moment (M_2) were included in the analysis because for these columns δ_{ns} exceeded 1.0. As a result, the analysis presented here includes data for 2168 of the 2960 frames initially used for this study. For load cases 1, 2, 3 and 4, the first-order end eccentricity ratio (e/h = $M_2/P_{u(th)}$h) ranges from 0.013 to 0.192 and the end moment ratio (M_1/M_2) is equal to -0.5 or 0.0 when the upper

end of the column is fix-ended or pin-ended, respectively. Therefore, the effects of e/h and M_1/M_2 on the strength ratio ($P_{u(th)}/P_{u(des)}$) will not be shown for load cases 1 to 4, because no trends were readily visible in the ranges of e/h and M_1/M_2 studied. Furthermore, as the beam bending moment ratio ($M_{bm}/M_{y(bm)}$) displayed little effect on the strength ratios of columns in frames subjected to load cases 1 to 4 or to load cases 5 to 6 within the range of $M_{bm}/M_{y(bm)}$ studied (0.84 to 1.12), those plots will not be shown for any of the load cases.

The effect of column slenderness ratio ($K\ell/r$) on the column strength ratio is examined in Figure 4. This figure was prepared for load cases 1 to 4 combined involving 648 reinforced concrete frames, where the theoretically computed maximum magnified bending moment due to second-order effects along the column height was greater than M_2. Note that, for computing the strength ratios shown in Figure 4, $P_{u(des)}$ was determined using the CSA A23.3-04 procedure for δ_{ns} (Eq. 1) and one of the following two equations for K: (a) the effective length factor from Eq. 2 (Jackson-Moreland Alignment Chart) for Figure 4(a); and (b) the effective length factor from Eq. 3 (Duan et al 1993) for Figure 4(b). Note also that, for the CSA moment magnifier procedure, δ_{ns} was calculated from axial loads and bending moments obtained from the conventional (first-order) elastic frame analysis.
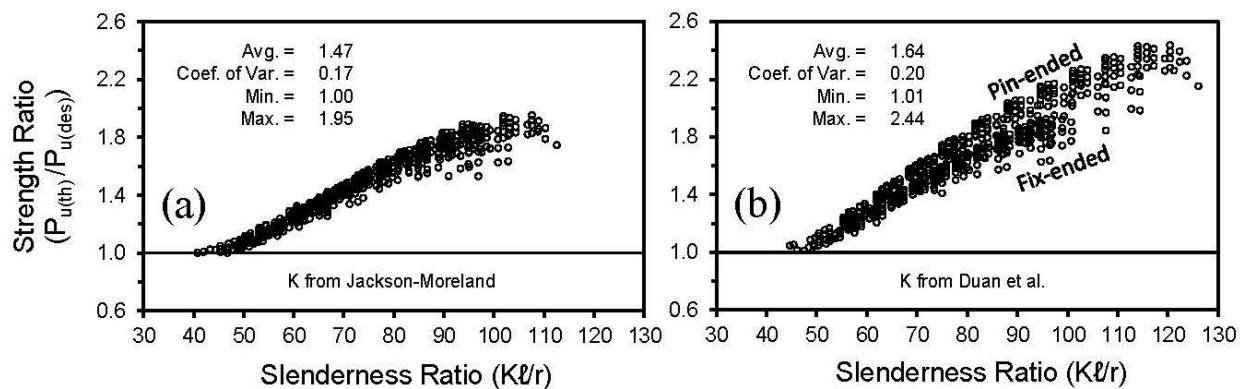

Figure 4: Effect of column slenderness ratio on strength ratios for load cases 1, 2, 3 and 4 (n = 648) calculated using (a) K from Jackson-Moreland Alignment Chart; and (b) K from Duan et al.

The strength ratios shown in Figure 4 indicate that both equations for K produce safe designs for all $K\ell/r$ values studied including for those that are beyond the upper limit of 100 placed on $K\ell/r$ by CSA A23.3-04 (2004). Figure 4(a), plotted using K from the Jackson-Moreland Alignment Chart, also shows that the strength ratios become increasingly conservative as $K\ell/r$ increases from approximately 40 to 110. Figure 4(b) was prepared from K based on the Duan et al. equation. A comparison of Figure 4(b) with Figure 4(a) shows that Figures 4(b) produces equally conservative albeit more scattered strength ratios than does Figure 4(a). This is expected because the Duan et al. equation computes more conservative values of K for pin-ended columns than those given by the Jackson-Moreland Alignment Chart, whereas both Jackson-Moreland Alignment Chart and Duan et al. equation compute very close values of K for fix-ended columns, as indicated by Figure 3. Consequently, Figure 4(b) shows two distinct groups of data, one for fix-ended and the other for pin-ended columns. Hence, Figure 4 leads to the conclusion that there appears to be no advantage in replacing the Jackson-Moreland Alignment Chart by the Duan et al. equation for the type of frames studied.

The effects of e/h, M_1/M_2, and $K\ell/r$ on the strength ratios for the combined data from load cases 5 and 6 are shown in Figures 5(a)-(f). These figures were plotted for 1520 reinforced concrete frames, where the theoretically computed maximum magnified moment due to second-order effects along the column height was greater than M_2. Consequently, as e/h increases from 0.1 to 1.0, the number of data points in Figures 5(a)-(f) decreases from 220 at e/h = 0.1 to 132 at e/h = 1.0. Note that M_1/M_2 ratio in these figures ranges from -0.4 (double curvature bending, $C_m = 0.44$) to 1.0 (single curvature bending, $C_m = 1.0$). For computing the strength ratios shown in Figures 5(a)-(f), $P_{u(des)}$ was determined using the CSA A23.3-04 procedure for δ_{ns} (Eq. 1) and one of the following two equations for K: (a) the effective length factor from Eq. 2 (Jackson-Moreland Alignment Chart) for Figures 5(a)-(c); and (b) the effective length factor from Eq. 3 (Duan et al. 1993) for Figures 5(d)-(f).

The strength ratios shown in Figures 5(a)-(c) for load cases 5 and 6 for which K was computed from the Jackson-Moreland Alignment Chart indicate a large spread in strength ratios. This is particularly valid for strength ratios with $e/h < 0.3$, $-0.3 < M_1/M_2 < 0.8$, and $K\ell/r > 70$, as indicated by Figures 5(a), 5(b), and 5(c), respectively. The Duan et al. equation was employed in place of the Jackson-Moreland Alignment Chart to calculate the K factor used in $P_{u(des)}$ for computing the strength ratios from load cases 5 and 6 plotted in Figures 5(d)-(f). A comparison of Figures 5(d)-(f) with Figures 5(a)-(c) shows a higher spread in strength ratios plotted in Figures 5(d)-(f), where the Duan et al. equation (Eq. 3) was used for computing K, as opposed to Figures 5(a)-(c) where the Jackson-Moreland Alignment Chart (Eq. 2) was employed for determining the K factor. However, both equations for K produced reasonably conservative strength ratios as indicated by Figures 5(a)-(f). This should be expected as explained earlier and indicates no advantage in replacing the Jackson-Moreland Alignment Chart with the Duan et al. equation for the types of frames studied.
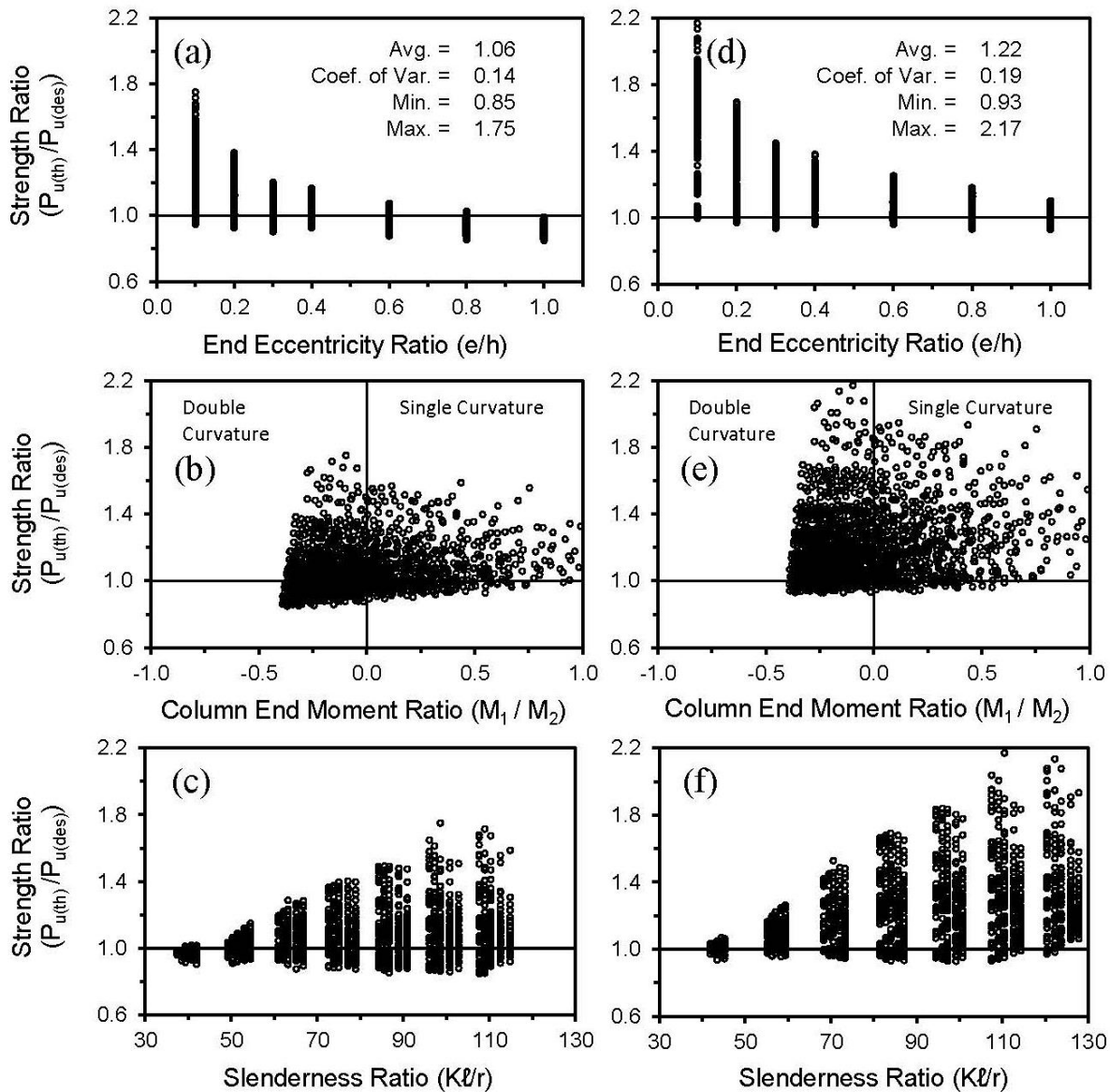

Figure 5: Effects of variables on strength ratios for load cases 5 and 6 (n = 1520) calculated using K from Jackson-Moreland Alignment Chart: (a) end eccentricity ratio (e/h), (b) column end moment ratio (M_1/M_2), (c) slenderness ratio ($K\ell/r$); and K from Duan et al. equation: (d) end eccentricity ratio (e/h), (e) column end moment ratio (M_1/M_2), (f) slenderness ratio ($K\ell/r$)

8. SUMMARY AND CONCLUSIONS

The CSA Standard A23.3-04 permits the use of the moment magnifier method for computing the ultimate strength of a slender reinforced concrete column. This computed CSA strength is influenced by the column effective length factor K, effective flexural stiffness EI, and the equivalent uniform bending moment diagram factor C_m among other factors. For this study, 2960 reinforced concrete non-sway frames in the shape of an inverted T subjected to short term loads were simulated to evaluate the accuracy of equations for K. The details of the simulated frames and variables used are discussed in Section 3. An elaborate theoretical strength model was developed and used for computing the ultimate strengths of columns in simulated frames. The theoretically computed column ultimate strengths were divided by the ultimate strengths of same columns calculated from the CSA moment magnifier method using different equations for K to obtain the nondimensionalized strength ratios. These strength ratios were statistically analyzed to evaluate the accuracy of K equations investigated. The materials and member resistance factors were taken equal to 1.0 for computing the CSA ultimate strengths. From the results presented in this paper, it is concluded that the Jackson-Moreland Alignment Chart is the most accurate of the selected equations available in the literature for computing the K factor. The results of the study are limited to non-sway frames in low-rise buildings.

REFERENCES

ACI. 2005. *Building Code Requirements for Structural Concrete (ACI 318-05) and Commentary (ACI 318R-05).* American Concrete Institute, Farmington Hills, Michigan, USA.

Bazant, Z.P., and Oh, B.H. 1984. Deformation of Progressively Cracking Reinforced Concrete Beams. *ACI Journal*, 81(3): 268-278.

Blomeier, G.A., and Breen, J.E. 1975. Effect of Yielding of Restraints on Slender Concrete Columns with Sidesway Prevented. *Reinforced Concrete Columns.* American Concrete Institute, Detroit, Michigan, USA, SP-50: 41-65

Breen, J.E., and Ferguson, P.M. 1964. The Restrained Long Concrete Column as a Part of a Rectangular Frame. *ACI Journal*, 61(5): 563-587.

CAC. 2006. Explanatory Notes on CSA Standard A23.3-04. *Concrete Design Handbook–Third Edition*, Cement Association of Canada, Ottawa, Ontario, Canada: 217-358.

Cranston, W. B. 1972. *Analysis and Design of Reinforced Concrete Columns (Research Report No. 20, Paper 41.020).* Cement and Concrete Association, London, UK.

CSA. 2004. *Design of Concrete Structures (CSA Standard A23.3-04).* Canadian Standards Association, Mississauga, Ontario, Canada.

Duan, L., King, W.S., and Chen, W. F. 1993. K-Factor Equation to Alignment Charts for Column Design. *ACI Structural Journal*, 90(3): 242-248.

Furlong, R.W., and Ferguson, P.M. 1966. Tests of Frames with Columns in Single Curvature. *Symposium on Reinforced Concrete Columns.* American Concrete Institute, Detroit, Michigan, USA, SP-13: 55-73.

Mirza, S.A., and MacGregor, J.G. 1989. Slenderness and Strength Reliability of Reinforced Concrete Columns. *ACI Structural Journal*, 86(4): 428-438.

Park, R., Priestly, M.J.N., and Gill, W.D. 1982. Ductility of Square-Confined Concrete Columns. *Journal of Structural Division*, ASCE, 108(ST4): 929-950.

Tikka, T.K., and Mirza, S.A. 2014. Effective Length of Reinforced Concrete Columns in Braced Frames. *International Journal of Concrete Structures and Materials*, 8(2): 99-116 (published at Springerlink.com).

Yalcin, C. and Saatcioglu, M. 2000. Inelastic Analysis of Reinforced Concrete Columns. *Computers and Structures*, 77(5): 539-555.